Pergamon

Int. J. Solids Structures Vol. 34, No. 3, pp. 341–357, 1997

0020–7683/97 $15.00 + .00

PII: S0020–7683(96)00020–0

BUCKLING OF MODERATELY THICK ORTHOTROPIC COLUMNS: COMPARISON OF AN ELASTICITY SOLUTION WITH THE EULER AND ENGESSER/HARINGX/TIMOSHENKO FORMULAE

G. A. KARDOMATEAS and D. S. DANCILA
School of Aerospace Engineering, Georgia Institute of Technology, Atlanta, Georgia 30332-0150, U.S.A.

(*Received* 14 *June* 1995; *in revised form* 12 *January* 1996)

Abstract—The objective of this paper is to answer the question of how accurately the simple Euler or transverse shear correction Engesser/Haringx/Timoshenko column buckling formulae are, when orthotropic composite material and moderate thickness are involved. The column is in the form of a hollow circular cylinder and the Euler or Timoshenko loads are based on the axial modulus. For this purpose, a three-dimensional elasticity solution is presented. As an example, the cases of an orthotropic material with stiffness constants typical of glass/epoxy or graphite/epoxy and the reinforcing direction along the periphery or along the cylinder axis are considered. First, it is found that the elasticity approach predicts in all cases a lower than the Euler value critical load. Moreover, the degree of non-conservatism of the Euler formula is strongly dependent on the reinforcing direction; the axially reinforced columns show the highest deviation from the elasticity value. The degree of non-conservatism of the Euler load for the circumferentially reinforced columns is much smaller and is comparable to that of isotropic columns. Second, the Engesser or first Timoshenko shear correction formula is in all cases examined conservative, i.e., it predicts a lower critical load than the elasticity solution. The Haringx or second Timoshenko shear correction formula is in most cases (but not always) conservative. However, in all cases considered, the second estimate is always closer to the elasticity solution than the first one. For the isotropic case both Timoshenko formulas are conservative estimates. Examination of a new formula for column buckling that adds a second term to the Euler load expression and is supposed to account for thickness effects, shows that this estimate is a non-conservative estimate but performs very well with very thick sections, being closest to the elasticity solution, but in general no better than the Timoshenko formulas for moderate thickness.

1. INTRODUCTION

The thrust of the initial applications of fiber reinforced composite materials was thin plate construction for aircraft parts. However, much attention is now being paid to configurations classified as moderately thick column-type structures. Such designs can be used, for example, as support members in civil and offshore structures, as well as for suspension and powertrain components in automobiles. Moreover, composite laminates have been considered in space vehicles in the form of circular cylinders as a primary load carrying structure.

In composite structural members, the buckling strength is an important design parameter because of the large strength-to-weight ratio and the lack of extensive plastic yielding in these materials. The case of a slender, ideal column, which is built in vertically at the base, free at the upper end, and subjected to an axial force P, constitutes the first problem of bifurcation buckling, the one that was originally solved by Euler (1744, 1933). The Euler solution is based on the well known Euler-Bernoulli assumptions (i.e., plane sections remain plane after bending, no effect of transverse shear) and for an isotropic elastic material. Nontrivial solutions (nonzero transverse deflections) are then sought for the equations governing bending of the column under an axial compressive load, and subject to the particular set of boundary conditions; thus, the problem is reduced to an eigen-boundary-value problem (e.g., Simitses, 1986).

Columns made out of composite materials for structural applications are envisioned in the form of a hollow cylinder of moderate thickness, produced mainly by filament

winding or pultrusion. Composite materials have one important distinguishing feature, namely extensional-to-shear modulus ratio much larger than that of their metal counterparts. The resulting effects of transverse shear may render the calculations of the critical load from simple classical column formulas highly non-conservative. Moreover, an additional deviation is expected because composites are anisotropic and these classical column formulae are based on isotropic material assumption. The objective of the present paper is to investigate the extent to which the classical Euler load represents the critical load, as derived by three dimensional elasticity analyses for a generally orthotropic rod with no restrictive assumptions regarding the cross sectional dimensions.

In a related article, Kardomateas (1993a) presented a three-dimensional elasticity formulation and solution for the problem of buckling of cylindrical orthotropic shells subjected to external pressure. It was shown that the critical load predicted by shell theory can be quite non-conservative for thick construction. This work was based on the simplifying assumption that the pre-buckling stress and displacement field was axisymmetric, and the buckling modes were assumed two dimensional (ring assumption), i.e., no z (axial) component of the displacement field, and no z-dependence of the r and θ displacement components. In a subsequent article, Kardomateas and Chung (1994) presented a solution that relaxes this ring approximation, i.e., based on a nonzero axial displacement and a full dependence of the buckling modes on the three coordinates.

Another investigation of the thickness effects was conducted by Kardomateas (1993b) for the case of a transversely isotropic thick cylindrical shell under axial compression. The reason for restricting the material to transversely isotropic was the desire to produce closed form analytical solutions. In a subsequent paper (Kardomateas, 1995a), the study was extended to the case of a generally orthotropic moderately thick shell under axial compression. A comparison with various shell theories showed that for the isotropic material cases considered, both the Flügge (1960) and Danielson and Simmonds (1969) shell theories predicted critical loads much closer to the elasticity value than the Donnell (Brush and Almroth, 1975) theory; the elasticity approach predicted a lower critical load than all these classical shell theories, the percentage reduction being larger with increasing thickness. However, in that study, an additional shell theory, namely that of Timoshenko and Gere (1961), was examined. It was found that for both the orthotropic and the isotropic material cases, the Timoshenko bifurcation points are lower than the elasticity ones. This means that the Timoshenko formulation is conservative, unlike all the other shell theories examined.

Finite element studies for thick and/or laminated beam structures are also an object of current interest. Improved kinematic approaches are called for because the classical beam assumptions which postulate that planes normal to the beam axis before deformation retain their planeness and normality, are violated. A variety of elements, based primarily on an assumed high order in terms of thickness power have been proposed in the literature. Recent work by Sheinman *et al.* (1995) on the buckling of laminated plane frames has shown that the first order model with an appropriate shear correction factor yields results close to its higher-order counterparts. The study presented in this paper can be used as a benchmark for evaluating the performance of various finite element formulations in predicting column buckling.

Regarding the formulas for the stability loss of elastic bars, the only alternative direct expressions to the Euler load that exist in the literature are two formulas described by Timoshenko and Gere (1961). These are actually the Engesser (1891) and Haringx (1948, 49) formulae (Haringx obtained the formula in connection with helical springs and Timoshenko applied Haringx's approach to bars; Timoshenko also referred to the Haringx analysis as the "modified" approach). These two formulas will also be referred to in this paper as the first and second Timoshenko shear correction formulae. These formulae were intended to account for the influence of transverse shearing forces. The specific load expressions, denoted by P_{T1} and P_{T2}, are given in the Results section. Despite the simplicity of the derivation of these formulas, it will be seen that they perform remarkably well in accounting for the thickness effects as well as for the effects of a low ratio of shear versus extensional modulus.

In a more recent study, Kardomateas (1995b) conducted a study on the buckling of solid transversely isotropic rods. By performing a series expansion of the terms of the resulting characteristic equation from the elasticity formulation for the isotropic case, the Euler load was proven to be the solution in the first approximation; consideration of the second approximation gave direct expression for the correction to the Euler load, therefore defining a new, yet simple formula for column buckling, which herein will be referred to as the Euler load with a second term.

In view of possible structural applications of anisotropic columns with sizable thickness, it is desirable to conduct a comprehensive study of the performance of the Euler and Engesser/Haringx/Timoshenko column buckling formulae. Therefore, the study conducted in this paper includes specific results for the critical load and the buckling modes of a cylindrical column in the form of a hollow cylinder under axial compression for various ratios of length over external radius, L/R_2, and ratios of external over internal radii, R_2/R_1. The effect of the material orthotropy is examined by considering two material cases: glass/epoxy and graphite/epoxy, and with reinforcing direction either along the circumferential (θ) or along the axial (z) direction.

Again, the non-linear three dimensional theory of elasticity is appropriately formulated, and reduced to a standard eigenvalue problem for ordinary linear differential equations in terms of a single variable (the radial distance r), with the applied axial load P the parameter. The formulation employs the exact elasticity solution by Lekhnitskii (1963) for the pre-buckling state. A full dependence on r, θ and z of the buckling modes is assumed. The results from the elasticity formulation will be compared with the classical Euler load predictions and with the Engesser or Haringx column buckling with transverse shear correction formulas which are described in Timoshenko and Gere's (1961), as well as with the Euler load with a second term, as derived by Kardomateas (1995b). To this extent, the present paper also extends the latter one by treating the case of orthotropy rather than transverse isotropy and the more practical tubular section rather than a solid circular one.

2. FORMULATION

The equilibrium of a column, considered as a three dimensional elastic body, can be described in terms of the second Piola-Kirchhoff stress tensor Σ in the form

$$\mathrm{div}\,(\Sigma \cdot \mathbf{F}^{\mathrm{T}}) = 0, \tag{1a}$$

where $\mathbf{F}$ is the deformation gradient defined by

$$\mathbf{F} = \mathbf{I} + \mathrm{grad}\mathbf{V}, \tag{1b}$$

where $\mathbf{V}$ is the displacement vector and $\mathbf{I}$ is the identity tensor.

Notice that the strain tensor is defined by

$$\mathbf{E} = \tfrac{1}{2}(\mathbf{F}^{\mathrm{T}} \cdot \mathbf{F} - \mathbf{I}). \tag{1c}$$

Since we consider a circular section, we can employ cylindrical coordinates and we can specifically write the components of the deformation gradient $\mathbf{F}$ in terms of the linear strains:

$$e_{rr} = \frac{\partial u}{\partial r}, \quad e_{\theta\theta} = \frac{1}{r}\frac{\partial v}{\partial \theta} + \frac{u}{r}, \quad e_{zz} = \frac{\partial w}{\partial z}, \tag{2a}$$

$$e_{r\theta} = \frac{1}{r}\frac{\partial u}{\partial \theta} + \frac{\partial v}{\partial r} - \frac{v}{r}, \quad e_{rz} = \frac{\partial u}{\partial z} + \frac{\partial w}{\partial r}, \quad e_{\theta z} = \frac{\partial v}{\partial z} + \frac{1}{r}\frac{\partial w}{\partial \theta}, \tag{2b}$$

and the linear rotations:

$$2\omega_r = \frac{1}{r}\frac{\partial w}{\partial \theta} - \frac{\partial v}{\partial z}, \quad 2\omega_\theta = \frac{\partial u}{\partial z} - \frac{\partial w}{\partial r}, \quad 2\omega_z = \frac{\partial v}{\partial r} + \frac{v}{r} - \frac{1}{r}\frac{\partial u}{\partial \theta}, \tag{2c}$$

as follows:

$$\mathbf{F} = \begin{bmatrix} 1+e_{rr} & \frac{1}{2}e_{r\theta} - \omega_z & \frac{1}{2}e_{rz} + \omega_\theta \\ \frac{1}{2}e_{r\theta} + \omega_z & 1+e_{\theta\theta} & \frac{1}{2}e_{\theta z} - \omega_r \\ \frac{1}{2}e_{rz} - \omega_\theta & \frac{1}{2}e_{\theta z} + \omega_r & 1+e_{zz} \end{bmatrix} \tag{3}$$

At the critical load there are two possible infinitely close positions of equilibrium. Denoting by u_0, v_0, w_0 the r, θ and z components of the displacement corresponding to the primary position, a perturbed position is denoted by

$$u = u_0 + \alpha u_1\,; \quad v = v_0 + \alpha v_1\,; \quad w = w_0 + \alpha w_1, \tag{4a}$$

where α is an infinitesimally small quantity. Here, $\alpha u_1(r, \theta, z)$, $\alpha v_1(r, \theta, z)$, $\alpha w_1(r, \theta, z)$ are the displacements to which the points of the body must be subjected to shift them from the initial position of equilibrium to the new equilibrium position. The functions $u_1(r, \theta, z)$, $v_1(r, \theta, z)$, $w_1(r, \theta, z)$ are assumed finite and α is an infinitesimally small quantity independent of r, θ, z. Also, notice that, as was shown in Kardomateas (1993a), the linear strains (2) rather than the nonlinear ones can be used in the first order problem.

Substituting into the strain-displacement relations and then using the orthotropic stress strain relations gives

$$e_{ij} = e_{ij}^0 + \alpha e'_{ij} + \ldots; \quad \sigma_{ij} = \sigma_{ij}^0 + \alpha \sigma'_{ij} + \ldots \tag{4b}$$

Following Kardomateas (1993a), we obtain the following buckling equations:

$$\frac{\partial}{\partial r}(\sigma'_{rr} - \tau^0_{r\theta}\omega'_z + \tau^0_{rz}\omega'_\theta) + \frac{1}{r}\frac{\partial}{\partial \theta}(\tau'_{r\theta} - \sigma^0_{\theta\theta}\omega'_z + \tau^0_{\theta z}\omega'_\theta)$$
$$+ \frac{\partial}{\partial z}(\tau'_{rz} - \tau^0_{\theta z}\omega'_z + \sigma^0_{zz}\omega'_\theta) + \frac{1}{r}(\sigma'_{rr} - \sigma'_{\theta\theta} + \tau^0_{rz}\omega'_\theta + \tau^0_{\theta z}\omega'_r - 2\tau^0_{r\theta}\omega'_z) = 0, \tag{5a}$$

$$\frac{\partial}{\partial r}(\tau'_{r\theta} + \sigma^0_{rr}\omega'_z - \tau^0_{rz}\omega'_r) + \frac{1}{r}\frac{\partial}{\partial \theta}(\sigma'_{\theta\theta} + \tau^0_{r\theta}\omega'_z - \tau^0_{\theta z}\omega'_r)$$
$$+ \frac{\partial}{\partial z}(\tau'_{\theta z} + \tau^0_{rz}\omega'_z - \sigma^0_{zz}\omega'_r) + \frac{1}{r}(2\tau'_{r\theta} + \sigma^0_{rr}\omega'_z - \sigma^0_{\theta\theta}\omega'_z + \tau^0_{\theta z}\omega'_\theta - \tau^0_{rz}\omega'_r) = 0, \tag{5b}$$

$$\frac{\partial}{\partial r}(\tau'_{rz} - \sigma^0_{rr}\omega'_\theta + \tau^0_{r\theta}\omega'_r) + \frac{1}{r}\frac{\partial}{\partial \theta}(\tau'_{\theta z} - \tau^0_{r\theta}\omega'_\theta + \sigma^0_{\theta\theta}\omega'_r)$$
$$+ \frac{\partial}{\partial z}(\sigma'_{zz} - \tau^0_{rz}\omega'_\theta + \tau^0_{\theta z}\omega'_r) + \frac{1}{r}(\tau'_{rz} - \sigma^0_{rr}\omega'_\theta + \tau^0_{r\theta}\omega'_r) = 0. \tag{5c}$$

In the previous equations, σ^0_{ij} and ω^0_j are the values of σ_{ij} and ω_j at the initial equilibrium position, i.e., for $u = u_0$, $v = v_0$ and $w = w_0$, and σ'_{ij} and ω'_j are the values at the perturbed position, i.e., for $u = u_1$, $v = v_1$ and $w = w_1$.

The boundary conditions associated with (1a) can be expressed as:

$$(\mathbf{F} \cdot \Sigma^{\mathrm{T}}) \cdot \hat{\mathbf{N}} = \mathbf{t}(\mathbf{V}), \tag{6}$$

where $\mathbf{t}$ is the traction vector on the surface which has outward unit normal $\hat{\mathbf{N}} = (\hat{\mathbf{l}}, \hat{\mathbf{m}}, \hat{\mathbf{n}})$ before any deformation. The traction vector $\mathbf{t}$ depends on the displacement field

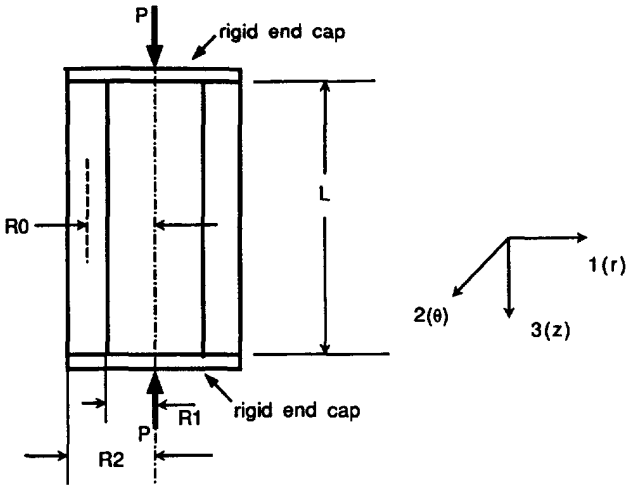

Fig. 1. Axially compressed column in the form of a hollow cylinder.

$\mathbf{V} = (u, v, w)$. Again, following Kardomateas (1993a), we obtain for the lateral and end surfaces:

$$(\sigma'_{rr} - \tau^0_{r\theta}\omega'_z + \tau^0_{rz}\omega'_\theta)\hat{\mathbf{l}} + (\tau'_{r\theta} - \sigma^0_{\theta\theta}\omega'_z + \tau^0_{\theta z}\omega'_\theta)\hat{\mathbf{m}} + (\tau'_{rz} - \tau^0_{\theta z}\omega'_z + \sigma^0_{zz}\omega'_\theta)\hat{\mathbf{n}} = 0, \tag{7a}$$

$$(\tau'_{r\theta} + \sigma^0_{rr}\omega'_z - \tau^0_{rz}\omega'_r)\hat{\mathbf{l}} + (\sigma'_{\theta\theta} + \tau^0_{r\theta}\omega'_z - \tau^0_{\theta z}\omega'_r)\hat{\mathbf{m}} + (\tau'_{\theta z} + \tau^0_{rz}\omega'_z - \sigma^0_{zz}\omega'_r)\hat{\mathbf{n}} = 0, \tag{7b}$$

$$(\tau'_{rz} + \tau^0_{r\theta}\omega'_r - \sigma^0_{rr}\omega'_\theta)\hat{\mathbf{l}} + (\tau'_{\theta z} + \sigma^0_{\theta\theta}\omega'_r - \tau^0_{r\theta}\omega'_\theta)\hat{\mathbf{m}} + (\sigma'_{zz} + \tau^0_{\theta z}\omega'_r - \tau^0_{rz}\omega'_\theta)\hat{\mathbf{n}} = 0. \tag{7c}$$

2.1. *Pre-buckling state*

The problem under consideration is that of an orthotropic hollow cylinder compressed by an axial force applied at one end. The stress-strain relations for the orthotropic body are

$$\begin{bmatrix} \sigma_{rr} \\ \sigma_{\theta\theta} \\ \sigma_{zz} \\ \tau_{\theta z} \\ \tau_{rz} \\ \tau_{r\theta} \end{bmatrix} = \begin{bmatrix} c_{11} & c_{12} & c_{13} & 0 & 0 & 0 \\ c_{12} & c_{22} & c_{23} & 0 & 0 & 0 \\ c_{13} & c_{23} & c_{33} & 0 & 0 & 0 \\ 0 & 0 & 0 & c_{44} & 0 & 0 \\ 0 & 0 & 0 & 0 & c_{55} & 0 \\ 0 & 0 & 0 & 0 & 0 & c_{66} \end{bmatrix} \begin{bmatrix} \varepsilon_{rr} \\ \varepsilon_{\theta\theta} \\ \varepsilon_{zz} \\ \gamma_{\theta z} \\ \gamma_{rz} \\ \gamma_{r\theta} \end{bmatrix}, \tag{8}$$

where c_{ij} are the stiffness constants (we have used the notation $1 \equiv r$, $2 \equiv \theta$, $3 \equiv z$).

Let R_1 be the internal and R_2 the external radius (Fig. 1).

Lekhnitskii (1963) gave the stress field for an applied compressive load of absolute value P, in terms of the quantities:

$$k = \sqrt{\frac{a_{11}a_{33} - a_{13}^2}{a_{22}a_{33} - a_{23}^2}}, \tag{9a}$$

$$\tilde{h} = \frac{(a_{23} - a_{13})a_{33}}{(a_{11} - a_{22})a_{33} + (a_{23}^2 - a_{13}^2)}. \tag{9b}$$

$$\tilde{T} = \pi(R_2^2 - R_1^2) - \frac{2\pi\tilde{h}}{a_{33}}\left[\frac{R_2^2 - R_1^2}{2}(a_{13}+a_{23}) - \frac{(R_2^{k+1} - R_1^{k+1})^2}{R_2^{2k} - R_1^{2k}}\frac{a_{13}+ka_{23}}{k+1}\right.$$
$$\left. - \frac{(R_2^{k-1} - R_1^{k-1})^2 (R_1 R_2)^2}{R_2^{2k} - R_1^{2k}}\frac{a_{13}-ka_{23}}{k-1}\right]. \quad (9c)$$

The stress field for orthotropy is as follows:

$$\sigma_{rr}^0 = P(C_0 + C_1 r^{k-1} + C_2 r^{-k-1}), \quad (10a)$$

$$\sigma_{\theta\theta}^0 = P(C_0 + C_1 k r^{k-1} - C_2 k r^{-k-1}), \quad (10b)$$

$$\sigma_{zz}^0 = -\frac{P}{\tilde{T}} - P\left(C_0\frac{a_{13}+a_{23}}{a_{33}} + C_1\frac{a_{13}+ka_{23}}{a_{33}}r^{k-1} + C_2\frac{a_{13}-ka_{23}}{a_{33}}r^{-k-1}\right), \quad (10c)$$

$$\tau_{r\theta}^0 = \tau_{rz}^0 = \tau_{\theta z}^0 = 0, \quad (10d)$$

where

$$C_0 = -\frac{\tilde{h}}{\tilde{T}}; \quad C_1 = \frac{R_2^{k+1} - R_1^{k+1}}{R_2^{2k} - R_1^{2k}}\frac{\tilde{h}}{\tilde{T}}, \quad (10e)$$

$$C_2 = \frac{R_2^{k-1} - R_1^{k-1}}{R_2^{2k} - R_1^{2k}}(R_1 R_2)^{k+1}\frac{\tilde{h}}{\tilde{T}}. \quad (10f)$$

Notice that for general orthotropy, both σ_{rr}^0 and $\sigma_{\theta\theta}^0$ are non-zero. For an isotropic or transversely isotropic body, these two stress components are zero.

In the previous equations a_{ij} are the compliance constants, i.e.,

$$\begin{bmatrix} \varepsilon_{rr} \\ \varepsilon_{\theta\theta} \\ \varepsilon_{zz} \\ \gamma_{\theta z} \\ \gamma_{rz} \\ \gamma_{r\theta} \end{bmatrix} = \begin{bmatrix} a_{11} & a_{12} & a_{13} & 0 & 0 & 0 \\ a_{12} & a_{22} & a_{23} & 0 & 0 & 0 \\ a_{13} & a_{23} & a_{33} & 0 & 0 & 0 \\ 0 & 0 & 0 & a_{44} & 0 & 0 \\ 0 & 0 & 0 & 0 & a_{55} & 0 \\ 0 & 0 & 0 & 0 & 0 & a_{66} \end{bmatrix} \begin{bmatrix} \sigma_{rr} \\ \sigma_{\theta\theta} \\ \sigma_{zz} \\ \tau_{\theta z} \\ \tau_{rz} \\ \tau_{r\theta} \end{bmatrix}. \quad (11)$$

2.2. *Perturbed state*

Using the constitutive relations (8) for the stresses σ'_{ij} in terms of the strains e'_{ij}, the strain-displacement relations (2) for the strains e'_{ij} and the rotations ω'_j in terms of the displacements u_1, v_1, w_1, and taking into account (10), the buckling eqn (5a) for the problem at hand is written in terms of the displacements at the perturbed state as follows:

$$c_{11}\left(u_{1,rr} + \frac{u_{1,r}}{r}\right) - c_{22}\frac{u_1}{r^2} + \left(c_{66} + \frac{\sigma_{\theta\theta}^0}{2}\right)\frac{u_{1,\theta\theta}}{r^2} + \left(c_{55} + \frac{\sigma_{zz}^0}{2}\right)u_{1,zz}$$
$$+ \left(c_{12} + c_{66} - \frac{\sigma_{\theta\theta}^0}{2}\right)\frac{v_{1,r\theta}}{r} - \left(c_{22} + c_{66} + \frac{\sigma_{\theta\theta}^0}{2}\right)\frac{v_{1,\theta}}{r^2}$$
$$+ \left(c_{13} + c_{55} - \frac{\sigma_{zz}^0}{2}\right)w_{1,rz} + (c_{13} - c_{23})\frac{w_{1,z}}{r} = 0. \quad (12a)$$

The second buckling eqn (5b) gives:

$$\left(c_{66}+\frac{\sigma_{rr}^0}{2}\right)\left(v_{1,rr}+\frac{v_{1,r}}{r}-\frac{v_1}{r^2}\right)+\left(\frac{\sigma_{rr}^0-\sigma_{\theta\theta}^0}{2}\right)\left(\frac{v_{1,r}}{r}+\frac{v_1}{r^2}\right)+c_{22}\frac{v_{1,\theta\theta}}{r^2}$$
$$+\left(c_{44}+\frac{\sigma_{zz}^0}{2}\right)v_{1,zz}+\left(c_{66}+c_{12}-\frac{\sigma_{rr}^0}{2}\right)\frac{u_{1,r\theta}}{r}+\left(c_{66}+c_{22}+\frac{\sigma_{\theta\theta}^0}{2}\right)\frac{u_{1,\theta}}{r^2}$$
$$+\left(c_{23}+c_{44}-\frac{\sigma_{zz}^0}{2}\right)\frac{w_{1,\theta z}}{r}+\frac{1}{2}\frac{\mathrm{d}\sigma_{rr}^0}{\mathrm{d}r}\left(v_{1,r}+\frac{v_1}{r}-\frac{u_{1,\theta}}{r}\right)=0. \quad (12b)$$

In a similar fashion, the third buckling eqn (5c) gives:

$$\left(c_{55}+\frac{\sigma_{rr}^0}{2}\right)\left(w_{1,rr}+\frac{w_{1,r}}{r}\right)+\left(c_{44}+\frac{\sigma_{\theta\theta}^0}{2}\right)\frac{w_{1,\theta\theta}}{r^2}+c_{33}w_{1,zz}$$
$$+\left(c_{13}+c_{55}-\frac{\sigma_{rr}^0}{2}\right)u_{1,rz}+\left(c_{23}+c_{55}-\frac{\sigma_{rr}^0}{2}\right)\frac{u_{1,z}}{r}$$
$$+\left(c_{23}+c_{44}-\frac{\sigma_{\theta\theta}^0}{2}\right)\frac{v_{1,\theta z}}{r}+\frac{1}{2}\frac{\mathrm{d}\sigma_{rr}^0}{\mathrm{d}r}(w_{1,r}-u_{1,z})=0. \quad (12c)$$

In the perturbed position, we seek equilibrium modes in the form:

$$u_1(r,\theta,z)=U(r)\cos\theta\sin\frac{\pi z}{L};\quad v_1(r,\theta,z)=V(r)\sin\theta\sin\frac{\pi z}{L},$$
$$w_1(r,\theta,z)=W(r)\cos\theta\cos\frac{\pi z}{L}, \quad (13)$$

where the functions $U(r)$, $V(r)$, $W(r)$ are uniquely determined. These equilibrium modes are the "column type" buckling modes of a single axial half-wave and circumferential wave. Figure 1 shows the geometry of the structure. Notice that the rigid end caps in the figure would simulate the freedom of nearly-rigid rotation (tilting) of the ends, which would most closely represent the displacement field in eqn (13) and, furthermore, would most closely represent the effect of the surrounding/connecting structure.

The equilibrium modes in eqn (13) are a special case of the general shell buckling modes:

$$u_1(r,\theta,z)=U(r)\cos n\theta\sin\frac{m\pi z}{L};\quad v_1(r,\theta,z)=V(r)\sin n\theta\sin\frac{m\pi z}{L},$$
$$w_1(r,\theta,z)=W(r)\cos n\theta\cos\frac{m\pi z}{L}, \quad (13a)$$

which had been considered in the three-dimensional elasticity shell buckling formulation of Kardomateas (1995a).

Notice that these modes correspond to the condition of "simply supported" ends since u_1 varies as $\sin\lambda z$ and

$$u_1=\frac{\mathrm{d}^2u_1}{\mathrm{d}z^2}=0 \quad \text{at } z=0,L.$$

Let now $U^{(i)}(r)$, $V^{(i)}(r)$ and $W^{(i)}(r)$ denote the i-th derivative of $U(r)$, $V(r)$ and $W(r)$ respectively, with the additional notation $U^{(0)}(r)=U(r)$, $V^{(0)}(r)=V(r)$ and $W^{(0)}(r)=W(r)$.

Substituting in (12a), we obtain the following linear homogeneous ordinary differential equation:

$$U(r)''c_{11}+U(r)'\frac{c_{11}}{r}+U(r)[(b_{00}+b_{01}P)r^{-2}+b_{02}Pr^{k-3}+b_{03}Pr^{-k-3}$$
$$+(b_{04}+b_{05}P)+b_{06}Pr^{k-1}+b_{07}Pr^{-k-1}]$$
$$+\sum_{i=0}^{1}V^{(i)}(r)[(d_{i0}+d_{i1}P)r^{i-2}+d_{i2}Pr^{k-3+i}+d_{i3}Pr^{-k-3+i}]$$
$$+\sum_{i=0}^{1}W^{(i)}(r)[(f_{i0}+f_{i1}P)r^{i-1}+f_{i2}Pr^{k-2+i}+f_{i3}Pr^{-k-2+i}]=0 \quad R_1\leqslant r\leqslant R_2. \tag{14a}$$

The second differential eqn (12b) gives:

$$V(r)[(g_{04}+g_{05}P)+g_{06}Pr^{k-1}+g_{07}Pr^{-k-1}]$$
$$+\sum_{i=0}^{2}V^{(i)}(r)[(g_{i0}+g_{i1}P)r^{i-2}+g_{i2}Pr^{k-3+i}+g_{i3}Pr^{-k-3+i}]$$
$$+\sum_{i=0}^{1}U^{(i)}(r)[(h_{i0}+h_{i1}P)r^{i-2}+h_{i2}Pr^{k-3+i}+h_{i3}Pr^{-k-3+i}]$$
$$+W(r)[(t_{00}+t_{01}P)r^{-1}+t_{02}Pr^{k-2}+t_{03}Pr^{-k-2}]=0 \quad R_1\leqslant r\leqslant R_2. \tag{14b}$$

In a similar fashion, (12c) gives:

$$W(r)q_{04}+\sum_{i=0}^{2}W^{(i)}(r)[(q_{i0}+q_{i1}P)r^{i-2}+q_{i2}Pr^{k-3+i}+q_{i3}Pr^{-k-3+i}]$$
$$+\sum_{i=0}^{1}U^{(i)}(r)[(s_{i0}+s_{i1}P)r^{i-1}+s_{i2}Pr^{k-2+i}+s_{i3}Pr^{-k-2+i}]$$
$$+V(r)[(\beta_{00}+\beta_{01}P)r^{-1}+\beta_{02}Pr^{k-2}+\beta_{03}Pr^{-k-2}]=0 \quad R_1\leqslant r\leqslant R_2. \tag{14c}$$

All the previous three eqns (14) are linear, homogeneous, ordinary differential equations of the second order for $U(r)$, $V(r)$ and $W(r)$. In these equations, the constants b_{ij}, d_{ij}, f_{ij}, g_{ij}, h_{ij}, t_{ij}, q_{ij}, s_{ij} and β_{ij} are given in the Appendix and depend on the material stiffness coefficients c_{ij} and k.

Now we proceed to the boundary conditions on the lateral surfaces $r=R_j$, $j=1,2$. These will complete the formulation of the eigenvalue problem for the critical load.

From (7), we obtain for $\hat{\mathbf{l}}=\pm 1$, $\hat{\mathbf{m}}=\hat{\mathbf{n}}=0$:

$$\sigma'_{rr}=0; \quad \tau'_{r\theta}+\sigma^0_{rr}\omega'_z=0; \quad \tau'_{rz}-\sigma^0_{rr}\omega'_\theta=0, \quad \text{at } r=R_1,R_2. \tag{15}$$

Substituting in (8), (2), (13), and (10), the boundary condition $\sigma'_{rr}=0$ at $r=R_j$, $j=1,2$ gives:

$$U'(R_j)c_{11}+[U(R_j)+V(R_j)]\frac{c_{12}}{R_j}-c_{13}\frac{\pi}{L}W(R_j)=0, \quad j=1,2. \tag{16a}$$

The boundary condition $\tau'_{r\theta}+\sigma^0_{rr}\omega'_z=0$ at $r=R_j$, $j=1,2$ gives

$$V'(R_j)\left[\left(c_{66}+\frac{C_0}{2}P\right)+\frac{C_1}{2}PR_j^{k-1}+\frac{C_2}{2}PR_j^{-k-1}\right]$$

$$+[V(R_j)+U(R_j)]\left[\left(-c_{66}+\frac{C_0}{2}P\right)R_j^{-1}+\frac{C_1}{2}PR_j^{k-2}+\frac{C_2}{2}PR_j^{-k-2}\right],\quad j=1,2. \tag{16b}$$

In a similar fashion, the condition $\tau'_{rz}-\sigma^0_{rr}\omega'_\theta=0$ at $r=R_j, j=1,2$ gives:

$$U(R_j)\frac{\pi}{L}\left[\left(c_{55}-\frac{C_0}{2}P\right)-\frac{C_1}{2}PR_j^{k-1}-\frac{C_2}{2}PR_j^{-k-1}\right]$$

$$+W'(R_j)\left[\left(c_{55}+\frac{C_0}{2}P\right)+\frac{C_1}{2}PR_j^{K-1}+\frac{C_2}{2}PR_j^{-k-1}\right],\quad j=1,2. \tag{16c}$$

Equations (14) and (16) constitute an eigenvalue problem for differential equations, with the applied compressive load P the parameter, which can be solved by standard numerical methods (two point boundary value problem).

Before discussing the numerical procedure used for solving this eigenvalue problem, one final point will be addressed. To completely satisfy all the elasticity requirements, we should discuss the boundary conditions at the ends. From (7), the boundary conditions on the ends are:

$$\tau'_{rz}+\sigma^0_{zz}\omega'_\theta=0;\quad \tau'_{\theta z}-\sigma^0_{zz}\omega'_r=0;\quad \sigma'_{zz}=0,\quad \text{at } z=0,L. \tag{17}$$

Since σ'_{zz} varies as $\sin(\pi/L)z$, the condition $\sigma'_{zz}=0$ on both the lower end $z=0$, and the upper end $z=L$, is satisfied.

In a cartesian coordinate system (x,y,z), the first two of the conditions in (17) can be written as follows:

$$\tau'_{xz}+\sigma^0_{zz}\omega'_y=0;\quad \tau'_{yz}-\sigma^0_{zz}\omega'_x=0. \tag{18}$$

It will be proved now that these remaining two conditions are satisfied on the average. At this point, it should be noted that for some of the boundary conditions, a form of resultant instead of pointwise conditions has been frequently used in elasticity treatments, and can be considered as based on some form of the Saint-Venant's principle. For this reason, they are sometimes referred to as relaxed end conditions of the Saint-Venant type (Horgan, 1989).

Now, the lateral surface boundary conditions in the cartesian coordinate system [analogous to (7)], with $\hat{\mathbf{N}}$ the normal to the circular contour are:

$$(\sigma'_{xx}-\tau^0_{xy}\omega'_z)\cos(\hat{\mathbf{N}},x)+(\tau'_{xy}-\sigma^0_{yy}\omega'_z)\cos(\hat{\mathbf{N}},y)=0, \tag{19a}$$

$$(\tau'_{xy}+\sigma^0_{xx}\omega'_z)\cos(\hat{\mathbf{N}},x)+(\sigma'_{yy}+\tau^0_{xy}\omega'_z)\cos(\hat{\mathbf{N}},y)=0. \tag{19b}$$

Using the equilibrium equation in cartesian coordinates [analogous to (5)], gives

$$\frac{\partial}{\partial z}\int\!\!\int_A(\tau'_{xz}+\sigma^0_{zz}\omega'_y)\,dA=-\int\!\!\int_A\left[\frac{\partial}{\partial x}(\sigma'_{xx}-\tau^0_{xy}\omega'_z)+\frac{\partial}{\partial y}(\tau'_{xy}-\sigma^0_{yy}\omega'_z)\right]dA. \tag{20a}$$

Using now the divergence theorem for transformation of an area integral into a contour integral, and the condition (19a) on the contour, gives the previous integral as

$$-\int_{\gamma}[(\sigma'_{xx}-\tau^0_{xy}\omega'_z)\cos(\hat{\mathbf{N}},x)+(\tau'_{xy}-\sigma^0_{yy}\omega'_z)\cos(\hat{\mathbf{N}},y)]\,\mathrm{d}s=0,$$

where A denotes the area of the annular cross section and γ the corresponding contour.

Therefore

$$\int\int_A(\tau'_{xz}+\sigma^0_{zz}\omega'_y)\,\mathrm{d}A=\text{const.} \tag{20b}$$

Since based on the buckling modes (13), τ'_{rz}, ω'_θ, $\tau'_{\theta z}$ and ω'_r and hence τ'_{xz}, ω'_y, τ'_{yz} and ω'_x, all have a $\cos(\pi z/L)$ variation, they become zero at $z=L/2$. Therefore, it is concluded that the constant in (20b) is zero. Similar arguments hold for τ'_{yz}.

Moreover, it can also be proved that the system of resultant stresses (18) would produce no torsional moment. Indeed,

$$\frac{\partial}{\partial z}\int\int_A[x(\tau'_{yz}-\sigma^0_{zz}\omega'_x)-y(\tau'_{xz}+\sigma^0_{zz}\omega'_y)]\,\mathrm{d}A=-\int\int_A\left\{x\left[\frac{\partial(\tau'_{xy}+\sigma^0_{xx}\omega'_z)}{\partial x}+\frac{\partial(\sigma'_{yy}+\tau^0_{xy}\omega'_z)}{\partial y}\right]-y\left[\frac{\partial(\sigma'_{xx}-\tau^0_{xy}\omega'_z)}{\partial x}+\frac{\partial(\tau'_{xy}-\sigma^0_{yy}\omega'_z)}{\partial y}\right]\right\}\mathrm{d}A$$

Again, using the divergence theorem, and taking into account (19), the previous integral becomes:

$$-\int_{\gamma}\{x[(\tau'_{xy}+\sigma^0_{xx}\omega'_z)\cos(\hat{\mathbf{N}},x)+(\sigma'_{yy}+\tau^0_{xy}\omega'_z)\cos(\hat{\mathbf{N}},y)]-y[(\sigma'_{xx}-\tau^0_{xy}\omega'_z)\cos(\hat{\mathbf{N}},x)+(\tau'_{xy}-\sigma^0_{yy}\omega'_z)\cos(\hat{\mathbf{N}},y)]\}\,\mathrm{d}s=0, \tag{21a}$$

hence

$$\int\int_A[x(\tau'_{yz}-\sigma^0_{zz}\omega'_x)-y(\tau'_{xz}+\sigma^0_{zz}\omega'_y)]\,\mathrm{d}A=\text{const}, \tag{21b}$$

and this constant is again zero since $\tau'_{xz}=\tau'_{yz}=\omega'_x=\omega'_y=0$ at $z=L/2$.

As has already been stated, eqns (14) and (16) constitute an eigenvalue problem for ordinary second order linear differential equations in the r variable, with the applied compressive load P the parameter. This is essentially a standard two point boundary value problem. The relaxation method was used (Press *et al.*, 1989) which is essentially based on replacing the system of ordinary differential equations by a set of finite difference equations on a grid of points that spans the entire thickness of the section. For this purpose, an equally spaced mesh of 241 points was employed and the procedure turned out to be highly efficient with rapid convergence. As an initial guess for the iteration process, the classical column theory solution was used. In the solution scheme, seven functions of r are defined as: $y_1=U$, $y_2=U'$, $y_3=V$, $y_4=V'$, $y_5=W$, $y_6=W'$ and $y_7=P$. The seven differential equations are: $y'_1=y_2$, eqn (14a), $y'_3=y_4$, eqn (14b), $y'_5=y_6$, eqn (14c), and $y'_7=0$. The corresponding seven boundary conditions are: at $r=R_2$ eqns (16a, b, c); at $r=R_2$ $U=1.0$; and at $r=R_1$ eqns (16a, b, c). The solution gives the eigenfunctions y_1, y_3, and y_5, as well as the eigenvalue y_7.

An investigation of the convergence showed that essentially the same results were produced with even three times as many mesh points. It is also first verified that the structure behaves as a column rather than a shell (which would buckle at multiple axial half-waves or circumferential waves). This is accomplished by considering the structure as a shell and

using the Kardomateas (1995a) solution to find if it would buckle at multiple axial half-waves or multiple circumferential waves. Finally, consideration of $n = 0$, $m = 1$ in eqn (13a) gives in all cases eigenvalues higher than for $n = 1$, $m = 1$ (which is the characteristic column buckling case).

3. DISCUSSION OF RESULTS

The Euler critical load for a compressed simply-supported column is:

$$P_{Euler} = \frac{\pi^2 E_3 I}{L^2} = E_3 I \lambda^2; \quad \lambda = \frac{\pi}{L}, \tag{22}$$

where I is the moment of inertia of the cross section.

Timoshenko describes two formulae that provide a correction to the Euler load due to the influence of transverse shearing forces. These formulae for the critical load, P_{T1} and P_{T2} are (Timoshenko and Gere, 1961):

$$P_{T1} = \frac{P_{Euler}}{1+\beta P_{Euler}/AG}, \tag{23}$$

$$P_{T2} = \frac{\sqrt{1+4\beta P_{Euler}/AG}-1}{2\beta/AG}, \tag{24}$$

where β is a numerical factor depending on the shape of the transverse section, A is the cross sectional area $[=\pi(R_2^2 - R_1^2)]$, and G is the shear modulus. For a tubular cross section, $\beta = 2.0$ (Gere and Timoshenko, 1990).

The first formula P_{T1} is actually the Engesser (1891) formula and second one P_{T2} is the formula obtained by Haringx (1948, 49) in connection with helical springs and applied by Timoshenko to bars.

By performing a series expansion of the terms of the resulting characteristic equation from the elasticity formulation for an isotropic column of solid circular cross section, Kardomateas (1995b) proved that the Euler load is the solution in the first approximation; consideration of the second approximation gave a direct expression for the correction to the Euler load, therefore defining a revised, yet simple formula for column buckling. Although this formula was derived by considering a solid cylinder, it can be heuristically extended for the case of a hollow cylinder. In terms of

$$\tilde{\lambda} = \lambda 2\sqrt{I/A} = \frac{\pi}{L}\sqrt{\frac{R_2^4 - R_1^4}{R_2^2 - R_1^2}}, \tag{25a}$$

and the Poisson's ratio, ν_{32}, the Euler load with a second term is:

$$P_{E2} = \lambda^2 E_3 I - \frac{\varepsilon_2}{16(1-\nu_{32}^2)} E_3 A, \tag{25b}$$

where

$$\varepsilon_2 = \sqrt{\Delta} - 4 - \frac{\tilde{\lambda}^2}{6}(5 + 2\nu_{32} + 12\nu_{32}^2), \tag{25c}$$

and

$$\Delta = 16 + \frac{\tilde{\lambda}^2}{3}(20 + 8\nu_{32} + 48\nu_{32}^2) + \frac{\tilde{\lambda}^4}{36}(409 + 212\nu_{32} - 356\nu_{32}^2 - 48\nu_{32}^3 + 144\nu_{32}^4). \quad (25d)$$

Results are produced for two common polymeric composites, namely the mildly orthotropic glass/epoxy and the strongly orthotropic graphic/epoxy. The elastic constants of the materials are given in the tables of the results, with the notation: 1, the radial (r), 2, the circumferential (θ) and 3, the axial (z) directions. Two reinforcing configurations are considered with each material, namely along the circumferential (θ) or along the axial (z) direction.

Regarding the glass/epoxy material, Tables 1a and 1b give the predictions of the Euler, P_{Euler}, the Engesser/Haringx/Timoshenko P_{T1} and P_{T2}, and the Euler with a second term, P_{E2}, formulae, as a ratio over the elasticity solution, P_{elast}, for radii ratio $R_2/R_1 = 1.20$, and column length ratios, L/R_2, ranging from 10 to 20. Tables 2a and 2b give the same data for graphite/epoxy material and Table 3 for isotropic material with Poisson's ratio $\nu = 0.300$.

Table 1. (a) Comparison with column buckling formulae. Glass/Epoxy with axial reinforcement, $R_2/R_1 = 1.20$ ($R_2 = 1.0$ m); moduli in GN/m^2: $E_2 = E_1 = 14$, $E_3 = 57$, $G_{31} = 5.7$, $G_{12} = 5.0$, $G_{23} = 5.7$; Poisson's ratios: $\nu_{12} = 0.400$, $\nu_{23} = 0.068$, $\nu_{31} = 0.277$

L/R_2	$P^{\dagger}_{Euler}/P_{elast}$	$P^{\dagger}_{T1}/P_{elast}$	$P^{\dagger}_{T2}/P_{elast}$	$P^{\dagger}_{E2}/P_{elast}$
10	1.598	0.870	1.036	1.502
12	1.414	0.894	1.002	1.354
14	1.304	0.914	0.986	1.263
16	1.232	0.929	0.978	1.203
18	1.183	0.941	0.976	1.161
20	1.149	0.950	0.975	1.131

† Column buckling formulae are based on the axial modulus; Euler load, eqn (22); Engesser and Haringx (also referred to as Timoshenko first and second formulas), eqns (23, 24) with $\beta = 2.0$; Euler formula with a second term, eqns (25).

Table 1. (b) Comparison with column buckling formulae. Glass/epoxy with circumferential reinforcement, $R_2/R_1 = 1.20$ ($R_2 = 1.0$ m); moduli in GN/m^2: $E_2 = 57$, $E_1 = E_3 = 14$, $G_{31} = 5.0$, $G_{12} = G_{23} = 5.7$; Poisson's ratios: $\nu_{12} = 0.068$, $\nu_{23} = 0.277$, $\nu_{31} = 0.400$

L/R_2	$P^{\dagger}_{Euler}/P_{elast}$	$P^{\dagger}_{T1}/P_{elast}$	$P^{\dagger}_{T2}/P_{elast}$	$P^{\dagger}_{E2}/P_{elast}$
10	1.145	0.950	0.974	1.081
12	1.100	0.963	0.976	1.057
14	1.073	0.971	0.979	1.042
16	1.056	0.977	0.982	1.032
18	1.044	0.982	0.985	1.025
20	1.035	0.985	0.987	1.020

† Column buckling formulae are based on the axial modulus; Euler load, eqn (22); Engesser and Haringx (also referred to as Timoshenko first and second formulas), eqns (23, 24) with $\beta = 2.0$; Euler formula with a second term, eqns (25).

Table 2. (a) Comparison with column buckling formulae. Graphite/Epoxy with axial reinforcement, $R_2/R_1 = 1.20$ ($R_2 = 1.0$ m); moduli in GN/m^2: $E_2 = 9.1$, $E_1 = 9.9$, $E_3 = 140.0$, $G_{31} = 4.7$, $G_{12} = 5.9$, $G_{23} = 4.3$; Poisson's ratios: $\nu_{12} = 0.533$, $\nu_{23} = 0.020$, $\nu_{31} = 0.283$

L/R_2	$P^{\dagger}_{Euler}/P_{elast}$	$P^{\dagger}_{T1}/P_{elast}$	$P^{\dagger}_{T2}/P_{elast}$	$P^{\dagger}_{E2}/P_{elast}$	
10	(3.948)	(1.061)	(1.775)	(3.711)	Buckles as a shell (2,3)‡
12	(2.751)	(0.952)	(1.401)	(2.634)	Buckles as a shell (2,3)‡
14	(2.023)	(0.847)	(1.136)	(1.959)	Buckles as a shell (2,4)‡
16	1.774	0.860	1.078	1.731	
18	1.612	0.876	1.044	1.581	
20	1.495	0.890	1.021	1.472	

† Column buckling formulae are based on the axial modulus; Euler load, eqn (22); Engesser and Haringx (also referred to as Timoshenko first and second formulas), eqns (23, 24) with $\beta = 2.0$; Euler formula with a second term, eqns (25).

‡(n, m) in eqn (13a) for the buckled modes.

Table 2. (b) Comparison with column buckling formulae. Graphite/Epoxy with circumferential reinforcement, $R_2/R_1 = 1.20$ ($R_2 = 1.0$ m); moduli in GN/m^2: $E_2 = 140$, $E_1 = 9.9$, $E_3 = 9.1$, $G_{31} = 5.9$, $G_{12} = 4.7$, $G_{23} = 4.3$; Poisson's ratios: $\nu_{12} = 0.020$, $\nu_{23} = 0.300$, $\nu_{31} = 0.490$

L/R_2	$P^{\dagger}_{Euler}/P_{elast}$	$P^{\dagger}_{T1}/P_{elast}$	$P^{\dagger}_{T2}/P_{elast}$	$P^{\dagger}_{E2}/P_{elast}$
10	1.121	0.952	0.972	1.060
12	1.081	0.963	0.974	1.040
14	1.058	0.970	0.976	1.028
16	1.042	0.975	0.979	1.020
18	1.032	0.978	0.981	1.014
20	1.024	0.981	0.982	1.010

† Column buckling formulae are based on the axial modulus; Euler load, eqn (22); Engesser and Haringx (also referred to as Timoshenko first and second formulas), eqns (23, 24) with $\beta = 2.0$; Euler formula with a second term, eqns (25).

Table 3. Comparison with column buckling formulae. Isotropic, $\nu = 0.300$, $R_2/R_1 = 1.20$ ($R_2 = 1.0$ m)

L/R_2	$P^{\dagger}_{Euler}/P_{elast}$	$P^{\dagger}_{T1}/P_{elast}$	$P^{\dagger}_{T2}/P_{elast}$	$P^{\dagger}_{E2}/P_{elast}$
10	1.137	0.934	0.960	1.068
12	1.095	0.951	0.966	1.048
14	1.069	0.963	0.972	1.036
16	1.053	0.971	0.976	1.028
18	1.042	0.976	0.980	1.022
20	1.034	0.981	0.983	1.018

† Euler load, eqn (22); Engesser and Haringx (also referred to as Timoshenko first and second formulas), eqns (23, 24) with $\beta = 2.0$; Euler formula with a second term, eqns (25).

The calculations for the critical loads from these formulas are based on the axial modulus, E_3. Finally, Table 4 performs an investigation of the effects of thickness by considering graphite/epoxy with circumferential reinforcement, a fixed length ratio $L/R_2 = 10$, and radii ratios R_2/R_1 ranging from 1.10 to 1.80. In all cases the external radius was kept constant at $R_2 = 1.0$ m. Specific conclusions from these results follow in the next section.

More insight into the variation of the critical load can be obtained from Figs 2 and 3, in which we have plotted the critical load vs the column length from all the different formulae, in comparison with the elasticity solution, for glass/epoxy with either circumferential or axial reinforcement. Data below the unit line are conservative estimates.

It should be emphasized at this point that the present paper is a single column-type mode treatment of a perfect rod, and compares with the Euler and Engesser/Haringx/Timoshenko formulae, which are also derived for a single-mode perfect rod; furthermore, all these treatments refer to the buckling (and not the post-critical) behavior. If the postbuckling behavior of the imperfect column were to be studied, however, mode interaction may become an issue for certain geometries for which shell-type phenomena

Table 4. Effect of thickness. Graphite/Epoxy with circumferential reinforcement, $R_2/R_1 = 10$ ($R_2 = 1.0$ m); moduli in GN/m^2; $E_2 = 140$, $E_1 = 9.9$, $E_3 = 9.1$, $G_{31} = 5.9$, $G_{12} = 4.7$, $G_{23} = 4.3$; Poisson's ratios: $\nu_{12} = 0.020$, $\nu_{23} = 0.300$, $\nu_{31} = 0.490$

L/R_2	$P^{\dagger}_{Euler}/P_{elast}$	$P^{\dagger}_{T1}/P_{elast}$	$P^{\dagger}_{T2}/P_{elast}$	$P^{\dagger}_{E2}/P_{elast}$
1.10	1.138	0.956	0.978	1.072
1.15	1.129	0.954	0.975	1.066
1.20	1.121	0.952	0.972	1.060
1.25	1.112	0.950	0.968	1.054
1.30	1.104	0.947	0.964	1.048
1.35	1.097	0.944	0.961	1.042
1.40	1.090	0.941	0.957	1.037
1.45	1.083	0.939	0.954	1.032
1.50	1.077	0.936	0.951	1.027

† Column buckling formulas are based on the axial modulus; Euler load, eqn (22); Engesser and Haringx (also referred to as Timoshenko first and second formulas), eqns (23, 24) with $\beta = 2.0$; Euler formula with a second term, eqns (25).

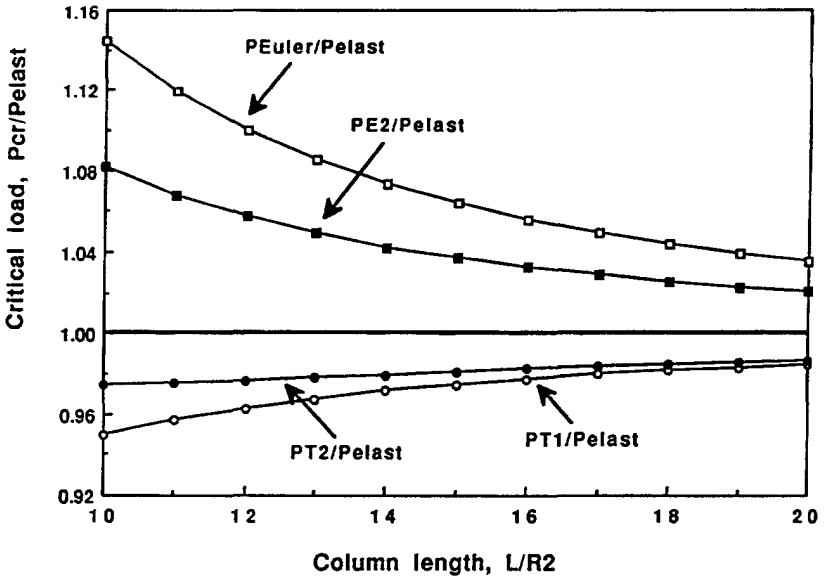

Fig. 2. The critical load from the Euler (PEuler), the Engesser or first Timoshenko (PT1), the Haringx or second Timoshenko (PT2), and the Euler with a second term (PE2) formulas, in comparison with the elasticity solution (Pelast) for the case of glass/Epoxy material with circumferential reinforcement. Data below the unit line are conservative estimates.

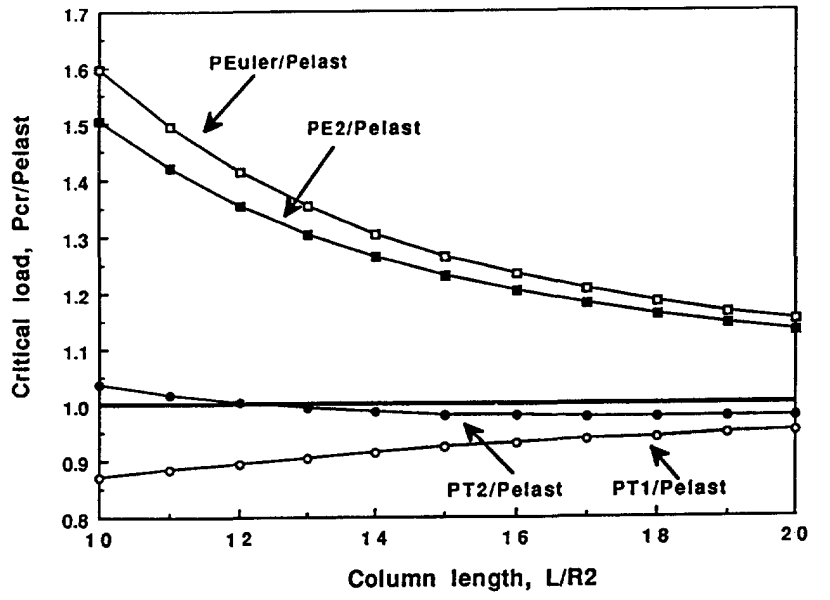

Fig. 3. The critical load from the Euler (PEuler), the Engesser or first Timoshenko (PT1), the Haringx or second Timoshenko (PT2), the Euler with a second term (PE2) formulas, in comparison with the elasticity solution (Pelast) for the case of glass/epoxy material with axial reinforcement.

could appear. In particular, it is well known that for imperfection-sensitive shells, there may exist several different buckling modes associated with the same or nearly the same critical load. Consequently, the different buckling modes may interact during the postcritical response and that may even cause the buckling modes to change from one mode to another at large deflections (e.g., the Yoshimura (1955) pattern). Other complicated interaction phenomena during post-buckling are those of the purely flexural and flexural-torsional overall modes of buckling with local buckling in thin walled columns (e.g., Ali and Sridharan, 1988).

Another important issue is that of the relation of compression strength to buckling strength. Indeed, in practical applications, the strength in compression has to be considered in conjunction with the results on the critical load, since compressive failure may precede buckling. For example, for the graphite epoxy with circumferential reinforcement (Table 2b), assuming a typical compressive strength of $\sigma_{cf} = 0.246$ GPa, the critical load P_{elast} is below the load corresponding to the compressive strength σ_{cf}, for length ratios L/R_2 beyond 12, which means that buckling would precede compressive failure. In some of the other configurations, compressive failure would precede buckling. Although this simple calculation does not take into account the complex phenomena of composite failure that would involve among others, the influence of layer/fiber waviness, it illustrates the importance of considering buckling in compressively loaded composite structures.

Next follows a list of conclusions, drawn from the results of Tables 1–4 and Figs 2–3.

4. CONCLUSIONS

(1) In all cases the elasticity solution predicts a lower than the Euler value critical load, i.e., P_{Euler} is a non-conservative estimate. Moreover, the degree of non-conservatism of the Euler formula is strongly dependent on the reinforcing direction; the axially reinforced columns show the highest deviation from the elasticity value. The degree of non-conservatism of the Euler load for the circumferentially reinforced columns is much smaller and is comparable to that of isotropic columns.

(2) The strongly orthotropic graphite/epoxy material shows much higher deviations from the elasticity solution than the glass/epoxy in the axially reinforced configuration; however the deviations from the elasticity solution for both the graphite/epoxy and glass/epoxy are comparable in the circumferentially reinforced case.

(3) For the small length ratios (L/R_2 between 10 and 14), the graphite/epoxy with axial reinforcement buckles as a shell, i.e., with n and m in eqn (13a) different than unity; this is not the case with the glass/epoxy material.

(4) The Engesser shear correction formula (also referred to in this paper as the first Timoshenko formula) is in all cases examined conservative, i.e., it predicts a lower critical load than the elasticity solution.

(5) The Haringx shear correction formula (also referred to in this paper as the second Timoshenko formula) is in most cases (but not always) conservative. For the isotropic case (Table 3) it is conservative. However, for a strongly orthotropic material (graphite/epoxy with axial reinforcement, Table 2a) or for relatively short columns (Table 1a) it may be non-conservative. Also, in all cases considered, the Haringx (second Timoshenko) shear correction estimate is always closer to the elasticity solution than the first one. The tubular shape shear factor $\beta = 2.0$ has been used in both shear correction formulae (23), (24).

(6) The Euler load with a second term formula, eqn (25b), which is supposed to account for thickness effects, is a non-conservative estimate; it performs very well with very thick sections (Table 4), being closest to the elasticity value, but in general no better than the Engesser/Haringx/Timoshenko formulas for moderate thickness. Both the Euler and the Euler with a second term formulas improve their predictions (i.e., they are closer to the elasticity solution) with increased thickness; this is because shell effects would appear for smaller thicknesses.

Acknowledgements—The financial support of the Office of Naval Research, Ship Structures and Systems, S&T Division, Grant N00014-91-J-1892, and the interest and encouragement of the Grant Monitor, Dr Y. D. S. Rajapakse, are both gratefully acknowledged. The authors would also like to acknowledge helpful discussions with Prof. Charles W. Bert of the University of Oklahoma in connection with the Engesser and Haringx formulae.

REFERENCES

Ali, M. A. and Sridharan, S. (1988). A versatile model for interactive buckling of columns and beam-columns. *Int. J. Solids Structures* **24**, 481–496.

Brush, D. O. and Almroth, B. O. (1975). *Buckling of Bars, Plates, and Shells*, McGraw-Hill, New York.

Danielson, D. A. and Simmonds, J. G. (1969). Accurate buckling equations for arbitrary and cylindrical elastic shells. *Int. J. Eng. Sci.* **7**, 459–468.
Engesser, F. (1891). Die Knickfestigheit gerader Stabe. *Zentralblatt der Bauverwaltung* **11**, 483–486.
Euler, L. (1933). *De Curvis Elasticis*, vol. 20, no. 58, Bruges, Belgium p. 1 (English translation of the book *Methodus Inveniendi Lineas Curvas Maximi Minimive Proprietate Gaudentes*, 1744, Lausanne).
Flügge, W. (1960). *Stresses in Shells*, Springer, Berlin, pp. 426–432.
Gere, J. M. and Timoshenko, S. P. (1990). *Mechanics of Materials*, PWS-KENT Publishing Company, Boston, pp. 692–694.
Haringx, J. A. (1948). On highly compressible helical springs and rubber rods, and their application for vibration-free mountings, I. *Phillips Research Reports*, Vol. 3, Eindhover, Holland, pp. 401–449.
Haringx, J. A. (1949). On highly compressible helical springs and rubber rods, and their application for vibration-free mountings, II. *Phillips Research Reports*, Vol. 4, Eindhover, Holland, pp. 49–80.
Horgan, C. O. (1989). Recent developments concerning Saint-Venant's principle: an update. *Appl. Mech. Rev.* **42**, 295–303.
Kardomateas, G. A. (1993a). Buckling of thick orthotropic cylindrical shells under external pressure. *J. Appl. Mech. ASME* **60**, 195–202.
Kardomateas, G. A. (1993b). Stability loss in thick transversely isotropic cylindrical shells under axial compression. *J. Appl. Mech. ASME* **60**, 506–513.
Kardomateas, G. A. (1995a). Bifurcation of equilibrium in thick orthotropic cylindrical shells under axial compression. *J. Appl. Mech. ASME* **62**, 43–52.
Kardomateas, G. A. (1995b). Three dimensional elasticity solution for the buckling of transversely isotropic rods: the Euler load revisited. *J. Appl. Mech. ASME* **62**, 346–355.
Kardomateas, G. A. and Chung, C. B. (1994). Buckling of thick orthotropic cylindrical shells under external pressure based on non-planar equilibrium modes. *Int. J. Solids Structures* **31**, 2195–2210.
Lekhnitskii, S. G. (1963). *Theory of Elasticity of an Anisotropic Elastic Body*, Holden Day, San Francisco.
Press, W. H., Flannery, B. P., Teukolsky, S. A. and Vetterling, W. T. (1989). *Numerical Recipes*, Cambridge University Press, Cambridge.
Sheinman, I., Eisenberger, M. and Bernstein, Y. (1995). High-order element for pre-buckling analysis of laminated plane frames. *Int. J. Num. Methods in Engng* (in press).
Simitses, G. J. (1986). *An Introduction to the Elastic Stability of Structures*, Krieger, Malabar, FL.
Timoshenko, S. P. and Gere, J. M. (1961). *Theory of Elastic Stability*, McGraw-Hill Co., New York.
Yoshimura, Y. (1955). On the mechanism of buckling of a circular shell under axial compression. *NACA Tech. Note No.* 1390.

APPENDIX

For convenience define

$$D_0 = -\frac{1}{\tilde{f}} - C_0 \frac{a_{13}+a_{23}}{a_{33}}; \quad \lambda = \pi/L, \tag{A1}$$

$$D_1 = -C_1 \frac{a_{13}+ka_{23}}{a_{33}}; \quad D_2 = -C_2 \frac{a_{13}-ka_{23}}{a_{33}}. \tag{A2}$$

The coefficients of the first differential eqn (14a) are:

$$b_{00} = -(c_{22}+c_{66}); \quad b_{01} = -C_0/2.0; \quad b_{02} = -C_1 k/2; \quad b_{03} = C_2 k/2$$
$$b_{04} = -c_{55}\lambda^2; \quad b_{05} = -D_0\lambda^2/2; \quad b_{06} = -D_1\lambda^2/2; \quad b_{07} = -D_2\lambda^2/2, \tag{A3}$$

$$d_{10} = (c_{12}+c_{66}); \quad d_{11} = -C_0/2; \quad d_{12} = -kC_1/2; \quad d_{13} = kC_2/2$$
$$d_{00} = -(c_{22}+c_{66}); \quad d_{01} = -C_0/2; \quad d_{02} = -kC_1/2; \quad d_{03} = kC_2/2, \tag{A4}$$

$$f_{10} = -\lambda(c_{13}+c_{55}); \quad f_{11} = \lambda D_0/2; \quad f_{12} = \lambda D_1/2; \quad f_{13} = \lambda D_2/2$$
$$f_{00} = \lambda(c_{23}-c_{13}); \quad f_{01} = f_{02} = f_{03} = 0. \tag{A5}$$

The coefficients of the second differential eqn (14b) are given as follows:

$$g_{20} = c_{66}; \quad g_{21} = C_0/2; \quad g_{22} = C_1/2; \quad g_{23} = C_2/2$$
$$g_{10} = c_{66}; \quad g_{11} = C_0/2; \quad g_{12} = C_1/2; \quad g_{13} = C_2/2$$
$$g_{00} = -(c_{22}+c_{66}); \quad g_{01} = -C_0/2; \quad g_{02} = -C_1/2; \quad g_{03} = -C_2/2$$
$$g_{04} = -c_{44}\lambda^2; \quad g_{05} = -D_0\lambda^2/2; \quad g_{06} = -D_1\lambda^2/2; \quad g_{07} = -D_2\lambda^2/2, \tag{A6}$$

$$h_{10} = -(c_{66}+c_{12}); \quad h_{11} = C_0/2; \quad h_{12} = C_1/2; \quad h_{13} = C_2/2$$
$$h_{00} = -(c_{22}+c_{66}); \quad h_{01} = -C_0/2; \quad h_{02} = -C_1/2; \quad h_{03} = -C_2/2, \tag{A7}$$

$$t_{00} = (c_{23}+c_{44})\lambda; \quad t_{01} = -\lambda D_0/2; \quad t_{02} = -\lambda D_1/2; \quad t_{03} = -\lambda D_2/2. \tag{A8}$$

Finally, the coefficients of the third differential eqn (14c) are:

$$q_{20} = c_{55}; \quad q_{21} = C_0/2; \quad q_{22} = C_1/2; \quad q_{23} = C_2/2$$

$$q_{10} = c_{55}; \quad q_{11} = C_0/2; \quad q_{12} = kC_1/2; \quad q_{13} = -kC_2/2$$

$$q_{00} = -c_{44}; \quad q_{01} = -C_0; \quad q_{02} = -kC_1/2; \quad q_{03} = kC_2/2; \quad q_{04} = -c_{33}\lambda^2, \tag{A9}$$

$$s_{10} = (c_{55}+c_{13})\lambda; \quad s_{11} = -\lambda C_0/2; \quad s_{12} = -\lambda C_1/2; \quad s_{13} = -\lambda C_2/2$$

$$s_{00} = (c_{23}+c_{55})\lambda; \quad s_{01} = -\lambda C_0/2; \quad s_{02} = -k\lambda C_1/2; \quad s_{03} = k\lambda C_2/2, \tag{A10}$$

$$\beta_{00} = (c_{23}+c_{44})\lambda; \quad \beta_{01} = -\lambda C_0/2; \quad \beta_{02} = -k\lambda C_1/2; \quad \beta_{03} = k\lambda C_2/2. \tag{A11}$$